Guido J. Reiss*

Two structurally related, hydrogen-bonded polymorphs of the zwitterionic complex trichlorido-((dimethylphosphoryl)methanaminium-κ*O*)zinc(II)

DOI 10.1515/mgmc-2015-0024
Received August 6, 2015; accepted October 19, 2015; previously published online November 17, 2015

Abstract: By the reaction of (dimethylphosphoryl)methanamine (*dpma*) with one equivalent of zinc(II) chloride in a hydrochloric acid solution and subsequent slow evaporation of the solvent, the title compound *dpma*$HZnCl_3$ was obtained in almost quantitative yield. The reaction product mainly consists of brick-shaped colorless crystals. Additionally, some smaller cuboid colorless crystals could be separated from the mother liquor. Structure analyses of two differently shaped crystals revealed that the block-shaped crystals **6a** show a monoclinic diffraction pattern with the space group $P2_1/c$, whereas the cuboid-shaped crystals **6b** possess tetragonal symmetry with the non-centrosymmetric space group $P4_1$. Both crystal structures consist of zwitterionic *dpma*$HZnCl_3$ complexes containing the cationic *dpma*H^+ ligand, which coordinates the zinc metal center through its oxygen atom. One more common feature of both structures is an intramolecular N-H···Cl hydrogen bond that fixes the conformation about the central P-C bond of the *dpma*H^+ ligand. The polymorphs differ with regard to their intermolecular hydrogen bonding schemes. In the structure of polymorph **6a**, one out of the two chlorido ligands, not involved in the intramolecular hydrogen bond, forms two N-H···Cl hydrogen bonds to aminium groups of two adjacent complexes, whereas the third chlorido ligand is uninvolved in any classical hydrogen bonding. This connection scheme constructs layers in the *ab* plane. In the crystal structure of polymorph **6b**, both chlorido ligands that are not involved in the intramolecular hydrogen bond form intermolecular NH···Cl connections. This connectivity scheme results in one-dimensional polymers running perpendicular to the *c* direction. Common to both structures is that each aminium group form three unbifurcated N-H···Cl hydrogen bonds.

Keywords: constructor graph; crystal structure; hydrogen bonding; polymorphism; zinc(II) complex.

Introduction

The first report on the syntheses and the structures of metal complex (Zn, Ni, Pd) containing the neutral (dimethylphosphoryl)methanamine (*dpma*) ligand dates back to the nineties of the last century (Dodoff et al., 1990). Since then, a series of related transition metal complexes have been characterized (Borisov et al., 1994; Kochel, 2009; Vornholt et al., 2014). It has also been shown that the N-protonated *dpma* ligand (*dpma*H^+) is able to form the transition metal complexes **1** (Reiss, 2013a; Richert et al., 2014) and **2** (Reiss, 2013b; Scheme 1). A search for structures in the Cambridge Structural Database (CSD) proved that the neutral complexes **3**, which compromise three halogenido and one *O*-coordinated phosphoryl moiety, are well known for trivalent metals (Dunbar et al., 1990; Burford, 1992; Vijjulatha et al., 1997; Aizawa et al., 2013). Only a few homologous anionic complexes **4** of divalent metals (Beagley et al., 1988; Muñoz et al., 1997; Exarchos et al., 2001) have been structurally characterized. The analogous copper(II) complex **5** (Newton et al., 1974; Marsh, 1997) is besides **2** a very rare example of a structurally characterized zwitterionic complex in this class of compounds (Scheme 1). The structure of an analogous zinc(II)-based zwitterionic complex **6** is unknown to the best of my knowledge.

Finally, it is worth mentioning that the *dpma*H^+ cation is an excellent tecton to construct hydrogen-bonded architectures. There are numerous examples of one-dimensional polymeric motifs in structures of simple *dpma*H^+ salts caused by the predominance of a head-to-tail connection of the aminium group and the phosphoryl moiety (Kessler and Reiss, 2014). Based on its conformational flexibility, the *dpma*H^+ tecton is able to fit with the needs of packing and hydrogen bonding even in complex structures (e.g. Reiss, 2013c). This contribution is part of my continuing interest on the construction of hydrogen-bonded architectures based on complex tectons.

***Corresponding author: Guido J. Reiss,** Institut für Anorganische Chemie und Strukturchemie, Lehrstuhl für Materialforschung, Heinrich-Heine-Universität Düsseldorf, D-40225 Düsseldorf, Germany, e-mail: reissg@hhu.de

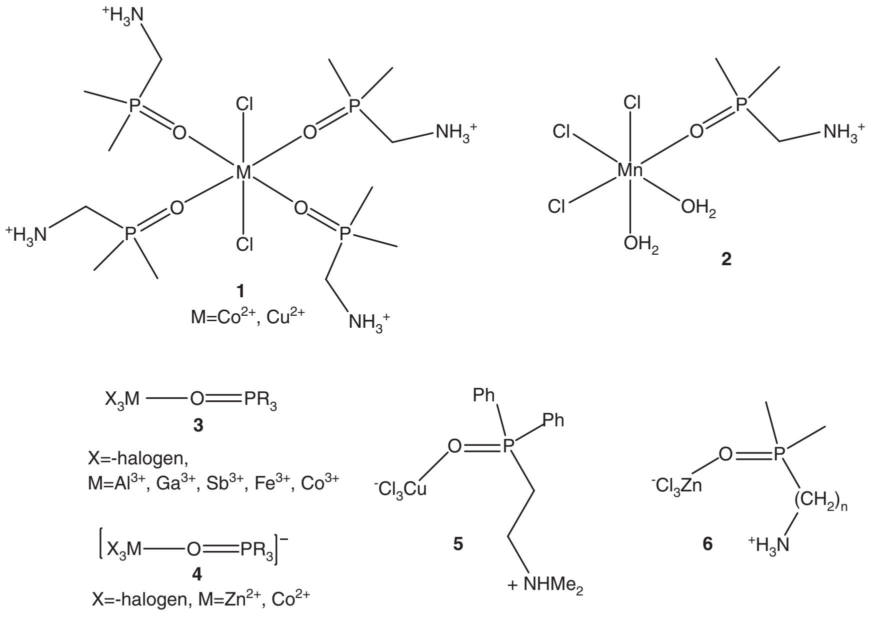

Scheme 1: Schematic drawings of *dpma*H$^+$-containing complexes of Cu(II) (**1**), Co(II) (**1**) and Mn(II) (**2**) and some trihalogenido complexes which furthermore coordinate to a phosphoryl moiety (**3**–**6**).

Results and discussion

The reaction of $ZnCl_2$ with *dpma* in a hydrochloric acid solution results in the crystalline material trichlorido(*dpma*H-κ*O*)zinc(II) (**6**). Two types of crystals can be distinguished optically. The majority of them are monocrystalline blocks with a monoclinic habitus (**6a**). Additionally, a limited number of tetragonally shaped, significantly smaller crystals are present (**6b**). The structural characterization of both specimens reveals that the title compound shows at least dimorphism.

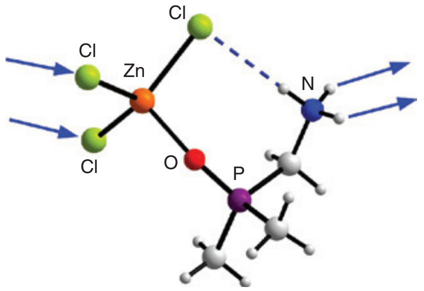

Figure 1: The title complex *dpma*H$ZnCl_3$ is shown with the intramolecular hydrogen bond. Arrows indicate the preferable directions for further hydrogen-bonding interactions of this supramolecular tecton. The graph-set descriptor for the intramolecular hydrogen bond is $S^1_1(7)$ (Grell et al., 1999).

Crystal structures

In both crystal structures **6a** and **6b**, the cationic *dpma*H$^+$ ligand coordinates to a formal negatively charged $ZnCl_3$ moiety. Also, in each structure, an intramolecular NH···Cl hydrogen bond, which is typical for the *dpma*H$^+$ ligand (Reiss, 2013a; Richert et al., 2014), leads to an eight-membered cyclic unit (Figure 1). The zwitterionic nature of this complex is clearly visible, as its cationic partial charge is located at the aminium group and the negative partial charge is distributed over the chlorido ligands. Caused by the intramolecular hydrogen bonds in both structures, the structural parameters of all crystallographically independent complex moieties are similar but not identical. In detail, in the structure of **6a**, the asymmetric unit contains one complete *dpma*H$ZnCl_3$ complex, whereas in **6b**, two crystallographically independent complexes are present (Figures 2 and 3, Tables 1 and 2). In the concept of crystal engineering of hydrogen-bonded structures, the title complex is a semi-rigid tecton that preferably accepts intermolecular hydrogen bonds at the $ZnCl_2$ moiety and donates hydrogen bonds by two of the hydrogen atoms of the NH_3^+ group (see blue arrows in Figure 1). We have already shown that the *dpma*H$^+$ tecton, which shows an analogous topology, tends to form structures with a head-to-tail connection as the predominant motif (Buhl et al., 2013; Kessler and Reiss, 2014).

The fine-tuning of the geometrical parameters of these *dpma*H$ZnCl_3$ tectons can be read from intramolecular

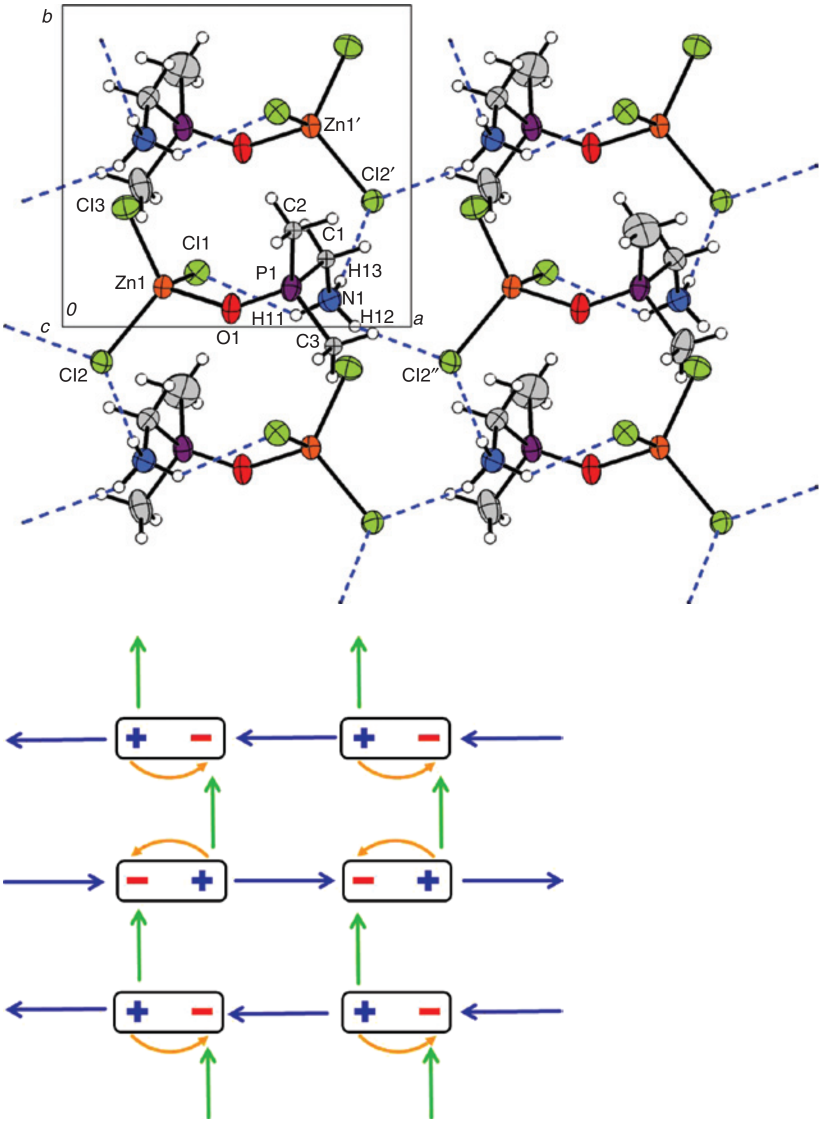

Figure 2: Upper part: the crystal structure of the monoclinic polymorph **6a** is shown along [00-1]. Hydrogen bonds are indicated by blue fragmented lines. Ellipsoids are drawn at the 40% probability level. Symmetry codes: ′=1-*x*, 0.5+*y*, 0.5-*z*; ″=1+*x*, *y*, *z*. Lower part: the constructor graph of the hydrogen-bonded connection of the title complex in **6a** is shown; crystallographically related hydrogen bonds are coded by their colors.

hydrogen bond distances (**6a**: N···Cl=3.2635(16) Å; **6b**: N···Cl=3.293(4) and 3.292(4) Å) and is depending on the structure they construct. According to the very similar values of the two crystallographically independent intramolecular hydrogen bonds, they are considered as identical for any further discussions. The intramolecular N···Cl as well as the intermolecular ones are significantly shorter than those found in related neutral $ZnCl_2L_2$ moieties, with ligands L able to donate hydrogen bonds (Vornholt et al., 2014; Kociok-Köhn et al., 2015). The coordination of the Zn metal centers in both structures is almost that of a distorted tetrahedron. In detail, in all moieties, the Zn-O distances are shorter than the Zn-Cl distances, and the O-Zn-Cl angles are smaller than the Cl-Zn-Cl angels (Table 1).

It should be noted here that there is also a specific biological interest on halogenido zinc complexes. Trihalogenido zinc(II) complexes with ligands such as N^6-furfuryladenine have been reported to have biological activity (Hošek et al., 2013). In a similar N^6-benzyl-adenine zinc(II) complex, an intramolecular halogenido···H–N hydrogen bond stabilizes the conformation of the complex in a manner analogous to that in the *dpma*$HZnCl_3$ complex (Jennifer et al., 2014).

In the monoclinic crystal structure of **6a**, one out of the two chlorido ligands and the two hydrogen atoms of the

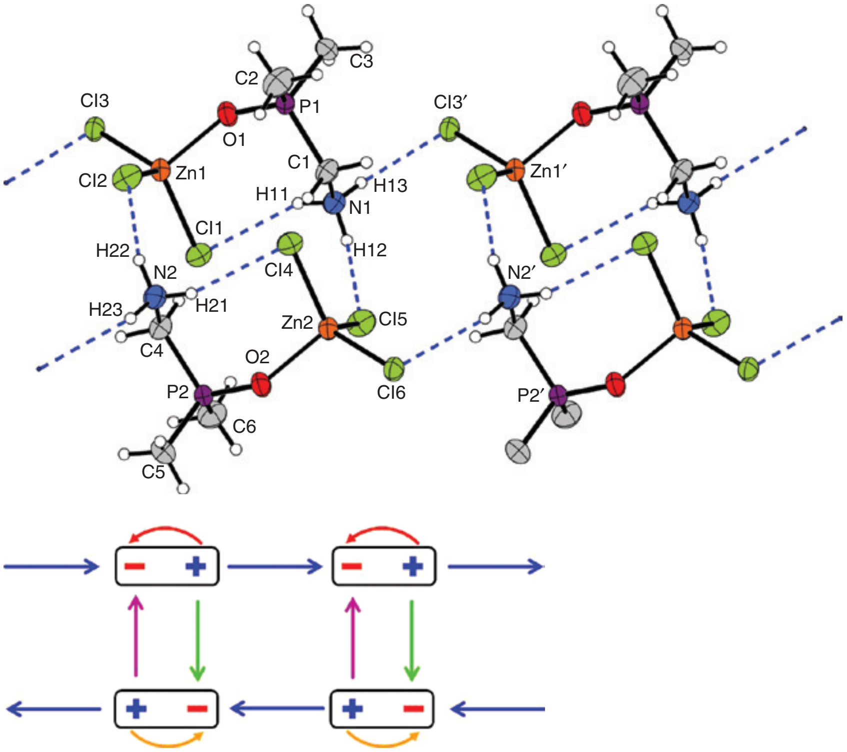

Figure 3: Upper part: the crystal structure of the tetragonal polymorph **6b** is shown. Hydrogen bonds are indicated by blue fragmented lines. Ellipsoids are drawn at the 40% probability level; symmetry code: ′=1+*x*, *y*, *z*. Lower part: constructor graph of the hydrogen-bonded connection of the title complex in **6b**; crystallographically related hydrogen bonds are coded by the colors.

Table 1: Selected bond lengths (Å) and angles (°) for **6a** and **6b**.

Polymorph **6a**			
Zn1-O1	1.9778(12)	Zn1-Cl1	2.2633(4)
Zn1-Cl2	2.2600(5)	Zn1-Cl3	2.2332(5)
O1-P1	1.4971(13)	P1-C1	1.8145(18)
C1-N1	1.471(2)		
O1-P1-C1	111.55(8)	P1-C1-N1	114.35(12)
O1-Zn1-Cl1	105.45(4)	O1-Zn1-Cl2	105.80(4)
O1-Zn1-Cl3	107.44(4)	Cl1-Zn1-Cl2	113.169(18)
Cl1-Zn1-Cl3	113.217(19)	Cl2-Zn1-Cl3	111.139(18)
C1-P1-O1-Zn1	-39.29(16)	N1-C1-P1-O1	-57.27(15)
Polymorph **6b**			
Zn1-O1	1.971(3)	Zn1-Cl1	2.2711(13)
Zn1-Cl2	2.2491(14)	Zn1-Cl3	2.2535(12)
O1-P1	1.496(3)	P1-C1	1.807(4)
C1-N1	1.483(6)	Zn2-O2	1.974(3)
Zn2-Cl4	2.2705(13)	Zn2-Cl5	2.2492(13)
Zn2-Cl6	2.2526(12)	O2-P2	1.501(3)
P2-C4	1.818(5)	C4-N2	1.467(6)
O1-P1-C1	110.0(2)	P1-C1-N1	114.4(3)
O1-Zn1-Cl1	104.52(11)	O1-Zn1-Cl2	104.52(11)
O1-Zn1-Cl3	104.23(10)	Cl1-Zn1-Cl2	114.73(5)
Cl1-Zn1-Cl3	114.08(5)	Cl2-Zn1-Cl3	110.85(5)
O2-P2-C4	109.6(2)	P2-C4-N2	114.3(3)
O2-Zn2-Cl4	107.06(11)	O2-Zn2-Cl5	103.99(10)
O2-Zn2-Cl6	104.07(11)	Cl4-Zn2-Cl5	113.98(5)
Cl4-Zn2-Cl6	115.73(5)	Cl5-Zn2-Cl6	110.72(5)
Zn1-O1-P1-C1	47.7(4)	O1-P1-C1-N1	50.7(4)
Zn2-O2-P2-C4	-50.7(4)	O2-P2-C4-N2	-48.6(4)

aminium group that are not involved in the intramolecular hydrogen bond form hydrogen bonds to four neighboring complexes (N1···Cl2′=3.1986; N1···Cl2″=3.2768(16) Å; Figure 2, upper part). These connections lead to a layered structure parallel to the *ab* plane.

In the tetragonal crystal structure of **6b**, each of the two crystallographically independent zinc(II) complexes form hydrogen-bonded connections by two chlorido ligands and the two hydrogen atoms of the aminium group, which are not involved in the intramolecular hydrogen bond, to three adjacent complexes (N1···Cl3′=3.229(4); N1···Cl5=3.222(4); N2···Cl2=3.220(4); N2′···Cl6=3.213(4) Å; Figure 3, upper part). Obviously, the intramolecular NH···Cl hydrogen bonds in the polymorph **6b** are with 3.293(4) and 3.292(4) Å, slightly longer than the one in **6a** (3.2635(16) Å). A finding which is in excellent agreement with only one intermolecular N···Cl distance below 3.25 Å in **6a** and two of them in **6b** for each crystallographically independent complex. Summing up the hydrogen bonding interactions in both polymorphs, the interaction quality is roughly the same, which may be the reason for their simultaneous occurrence. In line with these findings, the density of the polymorph **6a** is lower (Table 2).

Common to both structures is a head-to-tail connection of the zwitterionic complexes yielding a chain

Table 2: Crystallographic parameters.

Empirical formula	$C_3H_{11}Cl_3NOPZn$ (**6a**)	$C_3H_{11}Cl_3NOPZn$ (**6b**)
Formula weight	279.82	279.82
Temperature (K)	290	290
Wavelength (Å)	0.71073	0.71073
Crystal system	Monoclinic	Tetragonal
Space group	$P2_1/c$	$P4_1$
a (Å)	8.10969(9)	8.00101(9)
b (Å)	7.46091(10)	
c (Å)	17.9676(2)	33.5733(6)
β	93.364(1)	
Volume (Å^3)	1085.27(2)	2149.24(6)
Z	4	8
δ_c (g cm^{-3})	1.713	1.730
Absorption coefficient (mm^{-1})	3.095	3.126
Crystal size (mm)	0.18×0.30×0.46	0.19×0.30×0.43
θ range for data collection (°)	3.55–32.50	2.82–32.49
Reflections collected	74 847	62 649
Independent reflections	3930 [*R*(int)=0.0330]	7744 [*R*(int)=0.0374]
Reflections observed [$I>2\sigma I$]	3449	7227
Parameters/restraints	106/0	195/1
Goodness of fit	1.060	1.049
Final *R* indices [$I>2\sigma(I)$]	*R*1=0.0275	*R*1=0.0333
	w*R*2=0.0584	w*R*2=0.0645
R indices (all data)	*R*1=0.0335	*R*1=0.0368
	w*R*2=0.0613	w*R*2=0.0660
Largest diff. peak/hole (eA^{-3})	0.552/-0.516	0.598/-0.482
Flack–Parsons parameter[a]	–	0.026(3) (3205 quotients)

[a] Parsons et al. (2013).

structure as the primary motif (Figure 1). In the case of the layered, monoclinic polymorph **6a**, each hydrogen-bonded chain is connected to two neighboring ones. In the case of the tetragonal polymorph **6b**, chains are connected pairwise to form a complex chain structure along the *c* direction. For a better illustration of these similarities and differences of these complex hydrogen-bonded structures, the constructor graphs are shown (Figures 2 and 3, lower parts; Grell et al., 2002). Apart from my group's efforts, constructor graphs are rarely used (e.g. Guzei et al., 2010). Nonetheless, it is my considered view that they are useful tools to decode and compare complex hydrogen-bonded structures.

Spectroscopy

Usage of the attenuated total reflection (ATR) method allows the collection of infrared (IR) spectra from selected single crystals. Therefore, we sorted out some tetragonal and some monoclinic-shaped crystals for the IR experiments. For the Raman experiment, a larger amount of the compound was needed, representing a cross-section sample of both polymorphs. The IR absorption bands and Raman signals, which are typical for the *dpma*H$^+$ cation (Buhl et al., 2013), are present in the corresponding spectra (Figure 4). As discussed before, the geometric parameters of the zwitterionic complexes are very similar in both polymorphs. Consequently, the IR spectra of **6a** and **6b** are marginally different (Figure 4). The Raman spectrum does not allow an assignment of individual signals that are associated with -$ZnCl_3$ moiety. Summing up the number of crystallographically independent Zn-Cl distances equals to nine. For these bonds as well as for the three Zn-O bonds present in both polymorphs, stretching modes should be in the range between 350 and 200 cm^{-1}.

Conclusion

In the zwitterionic title complex trichlorido-((dimethylphosphoryl)methanaminium-κ*O*)zinc(II), the cationic *dpma*H$^+$ ligand coordinates the zinc(II) metal center with the oxygen atom. One more feature of this complex is the existence of an intramolecular N-H···Cl hydrogen bond, which fixes the conformation about the central P-C bond of the *dpma*H$^+$ ligand. It is shown that the title complex shows at least dimorphism. The two

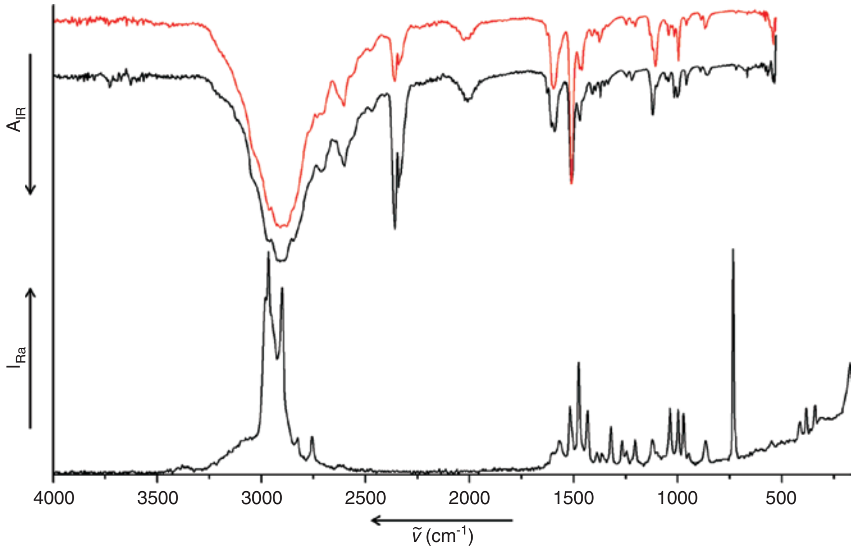

Figure 4: Upper part: IR spectra of the monoclinic polymorph **6a** (red) and of the tetragonal polymorph **6b** (black). Lower part: Raman spectrum of a cross-section sample of both polymorphs.

structurally related polymorphs **6a** and **6b** differ by their intramolecular connection via N-H···Cl hydrogen bonds. Their structural relation is visualized by the so-called constructor graphs (Grell et al., 2002).

Experimental

General

dpma can easily be obtained by a literature-known synthetic protocol (Tsvetkov et al., 1980; Varbanov et al., 1987). All other chemicals were obtained from commercial sources and were used as purchased.

Mid-IR spectra of some differently shaped crystals were selected and measured at room temperature on an Excalibur FTS 3500 spectrometer (Digilab, Germany) with an apodized resolution of 2 cm^{-1} using a MIRacle ATR unit (Pike Technologies, Madison, WI, USA) in the region of 4000–530 cm^{-1}. The Raman spectra of powder samples were recorded on a MultiRam spectrometer (Bruker Optics, Leipzig, Germany) with an apodized resolution of 8 cm^{-1} equipped with a Nd-YAG laser: 1064 nm and a RT-InGaAs detector in a backscattering geometry (4000–70 cm^{-1}, 128 scans, 10 mW). Elemental analysis (C, H, N) was recorded with a vario MICRO Cube instrument (Elementar Analysensystem GmbH, Hanau, Germany). The average value of the three measurements is given in the following. Not in all cases the viscos mother liquor can be removed completely resulting in a downward deviation.

Crystallography

All intensity data were collected with an Xcalibur CCD-diffractometer (Oxford Diffraction now a part of Rigaku) using Mo-Kα radiation at ambient temperature. Both structures were solved with direct methods using the SHELXS-97 program (Sheldrick, 2008), and all refinements were carried out using the SHELX-2014 program suite (Sheldrick, 2015). The C-H hydrogen atoms were positioned with idealized geometry and refined using a riding model. The hydrogen atoms at the aminium groups were included into the latest stages of the refinement using the AFIX 138 option of the SHELX program with their U_{iso} values refined freely. CCDC-1048499 and CCDC-1048505 contain the supplementary crystallographic data for this article. These data can be obtained free of charge from the Cambridge Crystallographic Data Centre via www.ccdc.cam.ac.uk/data_request/cif. The crystal data and the results of the structure refinement for both crystal structures presented in this contribution are shown in Table 2.

Synthesis

In a typical reaction, 0.54 g (0.5 mmol) of *dpma* and 0.68 g (0.5 mmol) of zinc(II) chloride were mixed and then stirred in 4 mL of concentrated hydrochloric acid and slowly heated until a colorless solution was obtained. Upon slow cooling to room temperature, colorless crystals formed. Crystals suitable for single crystal diffraction studies were grown at room temperature by slow evaporation. The majority of the crystals show a monoclinic habitus, whereas a few crystals are obviously tetragonally shaped. Anal. calcd. for $C_3H_{11}Cl_3NOPZn$ (%): C 12.88, H 3.96, N 5.01. Found: C 12.71, H 3.88, N 4.85.

Acknowledgments: I thank Elli Hammes and Martin van Megen for their technical support.

References

Aizawa, S.-i.; Fukumoto, K.; Kawamoto, T. Effect of phosphine and phosphine sulfide ligands on the cobalt-catalyzed reductive coupling of 2-iodobutane with *n*-butyl acrylate. *Polyhedron* **2013**, *62*, 37–41.

Beagley, B.; Benson, C. G.; Gott, G. A.; McAuliffe, C. A.; Pritchard, R. G.; Tanner, S. P. Some novel mixed tertiary phosphine-*t*-butyl isocyanide complexes of manganese(II): $[MnBr_2(CNBut)(PPhMe_2)]$ and $[Mn(CNBut)_4(PR_3)_2]^{2+}$ (PR_3=$PPhMe_2$, PPh_2Me, $PPhEt_2$, or $PPrn_3$), and the X-ray crystal structure of bis(dimethylphenylphosphine)tetrakis(t-butyl isocyanide) manganese(II) bis[tribromo(dimethylphenylphosphine oxide) manganate(II)], $[Mn(CNBut)_4(PPhMe_2)_2][MnBr_3(OPPhMe_2)]_2$. *J. Chem. Soc. Dalton* **1988**, *9*, 2261–2266.

Borisov, G.; Varbanov, S. G.; Venanzi, L. M.; Albinati, A.; Demartin, F. Coordination of dimethyl(aminomethyl)phosphine oxide with zinc(II), nickel(II), and palladium(II). *Inorg. Chem.* **1994**, *33*, 5430–5437.

Buhl, D.; Gün, H.; Jablonka, A.; Reiss, G. J. Synthesis, structure and spectroscopy of two structurally related hydrogen bonded compounds in the *dpma*/$HClO_4$ system; *dpma*=(dimethylphosphoryl)methanamine. *Crystals* **2013**, *3*, 350–362.

Burford, N. Modes of coordination for the phosphorylic unit. *Coord. Chem. Rev.* **1992**, *112*, 1–18.

Dodoff, N.; Macicek, J.; Angelova, O.; Varbanov, S. G.; Spassovska, N. Chromium(III), cobalt(II), nickel(II) and copper(II) complexes of (dimethylphosphinyl)-methanamine. Crystal structure of *fac*-tris{(dimethylphosphinyl)methanamine-N,O}nickel(II) chloride trihydrate. *J. Coord. Chem.* **1990**, *22*, 219–228.

Dunbar, K. R.; Haefner, S. C.; Quillevéré, A. Synthesis and characterization of $[\{2,4,6\text{-}(CH_3O)_3C_6H_2\}_3P{=}O]FeCl_3$: a four-coordinate phosphine oxide adduct of $FeCl_3$. *Polyhedron* **1990**, *14*, 1695–1702.

Exarchos, G.; Robinson, S. D.; Steed, J. W. The synthesis of new bimetallic complex salts by halide/sulfur chelate cross transfer: X-ray crystal structures of the salts $[Ni(S_2CNEt_2)(dppe)]_2[HgBr_4]$, $[Pt(S_2CNEt_2)(dppe)]_2[CdCl_4]$, $[Co(S_2CNEt_2)_2(dppe)]_2[Cl_3ZnO{:}(Ph)_2PCH_2CH_2P(Ph)_2{:}OZnCl_3]$ and $[Pd(S_2CN^nBu_2)(bipy)]_2[CdCl_4]$. *Polyhedron* **2001**, *20*, 2951–2963.

Grell, J.; Bernstein, J.; Tinhofer, G. Graph-set analysis of hydrogen-bond patterns: some mathematical concepts. *Acta Crystallogr.* **1999**, *B55*, 1030–1043.

Grell, J.; Bernstein, J.; Tinhofer, G. Investigation of hydrogen bond patterns: a review of mathematical tools for the graph set approach. *Crystallogr. Rev.* **2002**, *8*, 1–56.

Guzei, I. A.; Spencer, L. C.; Ainooson, M. K.; Darkwa, J. Constructor graph description of the hydrogen-bonding supramolecular assembly in two ionic compounds: 2-(pyrazol-1-yl)ethylammonium chloride and diaquadichloridobis(2-hydroxyethylammonium) cobalt(II) dichloride. *Acta Crystallogr*. **2010**, *C66*, m89–m96.

Hošek, J.; Novotná, R.; Babula, P.; Vančo, J.; Trávníček, Z. Zn(II)-Chlorido complexes of phytohormone kinetin and its derivatives modulate expression of inflammatory mediators in THP-1 cells. *PLoS One* **2013**, *8*, e65214.

Jennifer, S. J.; Muthiah, P. T.; Tamilselvi, D. Importance of halide involving interactions at Hoogsteen sites in supramolecular architectures of some coordination metal complexes of N6-benzyl/furfuryl adenine. *Chem. Cent. J.* **2014**, *8*, 58.

Kessler, D.; Reiss, G. J. Crystal structure of bis((dimethylphosphoryl) methanaminium) hexachloridoiridate(IV). *Z. Kristallogr. NCS* **2014**, *229*, 101–102 and references cited there.

Kochel, A. Synthesis and magnetic properties of the copper(II) complex derived from dimethyl aminomethylphosphine ox ideligand. X-ray crystal structure of DMAO and $[Cu(NO_3)_2(POC_3H_{10}N)_2]$. *Inorg. Chim. Acta* **2009**, *362*, 1379–1382.

Kociok-Köhn, G.; Molloy, K. C.; Sudlow, A. L. Synthesis and structure of zinc dichloride *bis*(t-butylhydrazine) monohydrate. *Main Group Met. Chem.* **2015**, *38*, 57–60.

Marsh, R. The perils of Cc revisited. *Acta Crystallogr.* **1997**, *B53*, 317–322.

Muñoz, A.; Escriche, J. L.; Casabó, J.; Pérez-Jiménez, C.; Kivekäs, R.; Sillanpää, R. A new pyridine-based phosphorus-containing macrocycle. Crystal structure of $[Co(\mathit{Lox})_2][CoCl_3(\mathit{Lox})]_2$ (*Lox*=6-phenyl-6-oxo-15-aza-6-phospha-3,9-dithiabicyclo[9,3,1] pentadeca-1(15),11,13-triene). *Inorg. Chim. Acta* **1997**, *257*, 99–104.

Newton, M. G.; Caughman, H. D.; Taylor, R. C. Synthesis and molecular structure of an inorganic zwitterion: trichloro{[2-(diphenylphosphinyl)ethyl]dimethylammonium}copper(II). *J. Chem. Soc. Dalton Trans.* **1974**, 1031–1037.

Parsons, S.; Flack, H. D.; Wagner, T. Use of intensity quotients and differences in absolute structure refinement. *Acta Crystallogr.* **2013**, *B69*, 249–259.

Reiss, G. J. *trans*-Dichlorido-tetrakis((dimethylphosphoryl) methanaminium)cobalt(II) bis(tetrachloridocobaltate(II)). *Acta Crystallogr.* **2013a**, *E69*, 248–249.

Reiss, G. J. The pseudosymmetric structure of *fac*-diaquatrichlori do((dimethylphosphoryl)methanaminium-κ*O*)manganese(II). *Acta Crystallogr.* **2013b**, *E69*, 250–251.

Reiss, G. J. The pseudosymmetric crystal structure of bis((dimethylphosphoryl)-methanaminium) oxonium tribromide. *Z. Kristallogr. NCS* **2013c**, *228*, 431–433.

Richert, M. E.; Reiss, G. J.; Helmbrecht, C. Synthesis, spectroscopy and crystal structure of a new copper complex built up by cationic (dimethylphosphoryl)methanaminium ligands. *Mediterran. J. Chem.* **2014**, *3*, 847–852.

Sheldrick, G. M. A short history of SHELX. *Acta Crystallogr.* **2008,** *A64*, 112–122.

Sheldrick, G. M. Crystal structure refinement with SHELXL. *Acta Crystallogr.* **2015,** *C71*, 3–8.

Tsvetkov, E. N.; Kron, T.E.; Kabachnik, M.I. Synthesis of chloromethylphosphine oxides. *Izv. Akad. Nauk. Ser. Khim.* **1980**, *3*, 669–672.

Varbanov, S. G.; Agopian, G.; Borisov, G. Polyurethane foams based on dimethylaminomethylphosphine oxides adducts with ethylene and propylene oxides. *Eur. Polym. J.* **1987**, *23*, 639–642.

Vijjulatha, M.; Kumara Swamy, K. C.; Huch, V.; Veith. M. The 1:1 antimony trichloride adduct of chlorobis(2,6-dimethylpiperidin-1-yl)phosphine oxide. *Acta Crystallogr.* **1997**, *C*53, 1789–1791.

Vornholt, S.; Herrmann, R.; Reiss, G. J. Crystal structure of the trinuclear complex hexachlorido-1k^3*Cl*,3κ^3*Cl*-bis(μ_2-dimethylphosphorylmethanamine-1:2κ^2 *N*:*O*,3:2 κ^2*N*:*O*)-bis(dimethylphosphorylmethanamine-2κ^2*N*,*O*) trizinc(II),$C_{12}H_{40}Cl_6N_4O_4P_4Zn_3$. *Z. Kristallogr. NCS* **2014**, *229*, 440–442.